General Disclaimer

One or more of the Following Statements may affect this Document

- This document has been reproduced from the best copy furnished by the organizational source. It is being released in the interest of making available as much information as possible.

- This document may contain data, which exceeds the sheet parameters. It was furnished in this condition by the organizational source and is the best copy available.

- This document may contain tone-on-tone or color graphs, charts and/or pictures, which have been reproduced in black and white.

- This document is paginated as submitted by the original source.

- Portions of this document are not fully legible due to the historical nature of some of the material. However, it is the best reproduction available from the original submission.

OLD DOMINION UNIVERSITY RESEARCH FOUNDATION

SCHOOL OF ENGINEERING
OLD DOMINION UNIVERSITY
NORFOLK, VIRGINIA

Technical Report 76-T3

LINEAR AND NONLINEAR ANALYSIS OF ORBITAL TELESCOPE/SPACE SHUTTLE DYNAMICS AND CONTROL

By

S.M. Joshi

Principal Investigator

A.S. Roberts, Jr.

Semi-annual Progress Report

Prepared for the
National Aeronautics and Space Administration
Langley Research Center
Hampton, Virginia

Under
Grant NSG 1241
September 15, 1975 - March 15, 1976

March 1976

TABLE OF CONTENTS

		Page
Summary		1
1.0	Introduction	1
	1.1 Symbols	5
2.0	Summary of Research Accomplishments	9
	2.1 Research Accomplishments	9
	2.2 Planned Publications	9
3.0	Mathematical Model Development	9
	3.1 Coordinate Systems	9
	3.2 Summary of Mathematical Model	10
	3.3 Kinetic Energy of the Shuttle	11
	3.4 Kinetic Energy of the Elevation Coarse Gimbal	12
	3.5 Kinetic Energy of the Lateral Coarse Gimbal	12
	3.6 Kinetic Energy of the Payload Assembly	13
	3.7 Generalized Forces	14
	3.8 Equations of Motion	15
4.0	Control Systems Design	19
	4.1 Coarse Gimbal Control Systems	19
	4.2 Magnetic Actuator Control Systems	21
	4.3 Space Shuttle Attitude Control System	23
5.0	Computational Aspects	23
	5.1 Equations of Motion When Actual Payload Parameters Differ From the Nominal	23
	5.2 Representation of Measurement Noise	26
6.0	Present and Future Efforts	28
Appendix		30
References		31

FIGURES

1.	Annular Suspension and Pointing (ASP) System	32
2.	Vernier Pointing Assembly Configuration	33

FIGURES (Concluded)

Page

3. Details of Coarse Pointing Assembly 34

4. Payload Assembly 35

LINEAR AND NONLINEAR ANALYSIS OF ORBITAL TELESCOPE/SPACE SHUTTLE DYNAMICS AND CONTROL

by

S.M. Joshi[1]

SUMMARY

During extended space shuttle orbital missions of the 1980's, a number of solar-, stellar-, and Earth-viewing scientific experiments shall be performed. These experiments require a highly accurate instrument pointing system for providing fine pointing in the presence of crew-motion and other disturbances, and sensor noise. In view of this, an annular suspension and pointing (ASP) system, which makes use of a magnetically suspended vernier pointing assembly, is being developed for ultimate implementation and flight testing, possibly during early space shuttle test flights. The objectives of this study are as follows:

- Development of a detailed mathematical model of the space shuttle/ASP system.
- Design of control laws in order to obtain the desired pointing performance.
- Prediction of the statiscal pointing accuracies in the presence of stochastic disturbances such as crew-motion, and sensor and actuator noise.

This report presents a part of the effort, consisting of linear analysis of the space shuttle/ASP system which is currently in progress. The material presented includes derivation of a mathematical model and design of appropriate control laws.

1. INTRODUCTION

During extended space shuttle orbital missions of the 1980's a number of solar-, stellar-, and Earth-viewing scientific experiments shall be performed.

---

[1]Research Assistant Professor in Electrical Engineering, Old Dominion University School of Engineering, Norfolk, Virginia 23508.

These experiments will require a highly accurate instrument pointing system for providing fine pointing in the presence of crew-motion and other disturbances. With this objective in mind, a concept for such an apparatus, an annular suspension and pointing (ASP) system, was conceived (ref. 1).

The annular suspension and pointing (ASP) system includes two assemblies with connecting interfaces, each assembly having a separate function. [See fig. 1(a).] The first assembly is attached to the carrier vehicle and consists of an azimuth gimbal and an elevation gimbal which provide "coarse" pointing of the payload instrument by allowing two rotations of the instrument relative to the carrier vehicle. For extensive Earth-pointing usage an alternative coarse gimbal arrangement [fig. 1(b)] may be preferable in which an elevation and a lateral gimbal provide simpler crosstrack capability when the space shuttle is in an inverted position relative to the local vertical. This coarse gimbal arrangement is assumed throughout this report. The second or vernier pointing assembly is made up of magnetic actuators for suspension and fine pointing, roll motor segments, and an instrument mounting plate around which a continuous annular rim (fig. 2) is attached which provides appropriate magnetic circuits for the actuators and the roll motor segments. The payload assembly, consisting of the payload instruments, the mounting surface, and the annular rim, is suspended in the elevation coarse gimbal without physical contact, and provides vernier attitude fine pointing and roll positioning of the instrument as well as six-degree-of-freedom isolation from carrier motion disturbances. In addition, the second assembly has a rim centering mode in which axial and radial rim position sensors located at each actuator station are used to center the rim axially and radially between actuator pole faces. This mode allows coarse gimbal slewing for retargeting, for Earth pointing, or for backup coarse gimbal pointing.

Nominal operation of the ASP system for solar or stellar pointing first involves coarse gimbal pointing with coarse (wide field of view) sensors onboard the ASP system (or with sensors onboard the carrier vehicle and relative gimbal angle information). The rim centering mode is activated during gimbal slewing. After coarse alinement, coarse roll positioning is accomplished by means of the rim roll motor and a relative roll sensor located on the rim together with a carrier sensor or a sensor onboard the ASP system. After coarse attitude alinement, vernier fine pointing is initiated. For this mode, errors obtained from fine (narrow field of view) attitude sensors located on the ASP system, either

as part of the instrument or remote, are nulled by small magnetic-suspension- and fine-pointing-actuator torques applied to the annular rim. Also, translation rim centering is accomplished for this mode.

Nominal operation of the ASP system for Earth pointing initially involves establishing the correct azimuth, elevation, and roll attitudes and attitude rates (slewing) in the rim centering mode. After appropriate smooth instrument slewing is established, vernier pointing (similar to that described for solar and stellar pointing) is accomplished.

The basic objectives of the present study are:

- Derivation of a detailed mathematical model of the space shuttle/ASP system.
- Design of control laws in order to obtain optimum performance.
- Prediction of the pointing performance when subjected to stochastic crew-motion and other disturbances, and sensor and actuator noise.

In reference 1, a linear mathematical model was developed for the space shuttle/ASP system. This model ignored the payload-to-shuttle coupling. Sensor noise and actuator noise were also ignored. An azimuth-elevation coarse gimbal configuration was used, and the coarse gimbals were assumed to be fixed relative to the shuttle. However, as pointed out earlier, the "elevation-lateral" coarse gimbal arrangement is more suitable, especially for Earth-viewing experiments, since it avoids gimbal lock. Therefore the present study assumes the latter coarse gimbal arrangement. The coarse gimbals are no longer fixed, and control systems are designed for moving the coarse gimbals in such a way as to minimize the summed norm of the magnetic suspension centering errors at the four magnetic bearing stations. The roll freedom and the magnetic roll actuators, which were not modeled in reference 1, will be included in the present study. Sensor noise and actuator noise are also included. The mathematical model obtained in the present study describes the system in considerable details. All the internal couplings, cross products of inertia, etc., are included in the model. This semiannual report deals mostly with Task 1 described in the original research proposal, namely, linear analysis and design.

Part 2 of this report contains a summary of research accomplishments and planned publications. Part 3 contains the derivation of a mathematical model using Lagrangian formulation. The design of controllers for the coarse gimbals

and the magnetic actuators is accomplished in part 4. Part 5 contains normalization of the equations of motion and inclusion of measurement noise and stochastic crew-motion model. Present and future research efforts are summarized in part 6.

1.1 Symbols

A, A_1, A_2, $\overline{A}$, $\overline{A}_1$, $\overline{A}_2$	System coefficient matrixes
A_2	Crew-motion filter coefficient matrix
A_j	Points on the payload assembly annular rim which correspond to the magnetic bearing stations on lateral coarse gimbal
A_{CF}, A'_{CF}	Magnetic force coefficient matrixes
a	Controller coefficient (rate gain)
A, A_i	Coefficient matrixes
B_1, B_{11}	System input matrixes
B_2	Crew-motion
B_j	Magnetic bearing stations on lateral coarse gimbal
b	Controller coefficient (proportional gain)
C_ζ	$-C_p\ (\zeta_{oq})$
C_1	$C_{\zeta_o} / \lvert\zeta\rvert$
$C_p\ (x)$	Cross-product matrix of vector x. $\left[x \times y = C_p\ (x)\ y\right]$
D_{AB}	Transformation matrix from A-coordinate system into B-coordinate system
E	Angular velocity transformation matrix defined in equation (2)
E_o	Normalized parameter matrix for the payload
e_j	Column vector containing all zeros except a "1" in the jth position
F_j	$(F_{xj}, F_{yj}, F_{zj})^T$, magnetic forces at the jth bearing station
F_c	Crew-motion force vector
F	(with other subscripts) generalized forces corresponding to the subscript coordinates
f_c	Normalized crew-motion force vector

g_1, g_2	Elevation and lateral coarse gimbals
H_{p_1}, H_{p_2s}, H_{oq}	Transformation matrixes
I	(with subscripts) Inertia matrix defined in equation (4)
I	(without subscript) Identity matrix
I_{xx}, I_{yy}, I_{xy}, etc.	Elements of Inertia matrix
J	Objective function
K_{g_1}, K_{g_2}	Coarse gimbal rate gains
L_{g_1}, L_{g_2}	Coarse gimbal proportional gains
m	$m_s + m_{g_1} + m_{g_2}$
m_s	Mass of the shuttle
m_{g_1}, m_{g_2}	Masses of coarse gimbals
m_p	Mass of payload
m_1	$mm_p/(m + m_p)$
O	Center of mass of payload
O_i	Origin of the coordinate system (X_i, Y_i, Z_i)
O_s	Center of mass of the shuttle
P_1	Origin of the coordinate system $(X_{g_1}, Y_{g_1}, Z_{g_1})$
P_2	Origin of the coordinate system $(X_{g_2}, Y_{g_2}, Z_{g_2})$
Q	Center of instrument mounting surface
q	Vector defined in equation (48)
q_r	Generalized coordinate
r	Radius of instrument mounting surface
T	Transformation matrix
T_1, T_2, T_3	Transformation matrices for 1, 2, 3 Eulerian rotations
T_s, T_{g_1}, T_{g_2}, T_p	Kinetic energies of shuttle, elevation gimbal, lateral gimbal and payload respectively

T_c	Crew-motion torque vector
T_{con}	Shuttle altitude control torque vector
t_c	Normalized crew-motion torque vector
u	White-noise source with unit power spectral density
$\overline{V}$	Noise covariance intensity matrix
v_{ABC}	Linear velocity of point "A" relative to B-coordinate frame, expressed along C-coordinates
$\overline{v}$	White noise vector
v_m	Measurement noise
x	State vector
(X_i, Y_i, Z_i)	Inertial coordinate system
$(X_{i_1}, Y_{i_1}, Z_{i_1})$	Inertial coordinate system
(X_s, Y_s, Z_s)	Coordinate system fixed to shuttle
$(X_{g_1}, Y_{g_1}, Z_{g_1})$	Coordinate system fixed to gimbal g_1
$(X_{g_2}, Y_{g_2}, Z_{g_2})$	Coordinate system fixed to gimbal g_2
(X_p, Y_p, Z_p)	Coordinate system fixed to payload, through its center of mass
(X_q, Y_q, Z_q)	Coordinate system fixed to payload through Q
α_s	Shuttle altitude vector
α_p, α_q	Payload altitude vectors
β_s	Normalized shuttle altitude vector
δ	Error variable
δ_j	(three-axis) centering errors at the jth magnetic bearing station
ε	Payload assembly position error
λ	Controller output
ν	Normalized payload assembly position error
ρ	(with subscripts) damping ratios

Σ	Covariance matrix of x
Σ_{ss}	Steady-state value of Σ
τ_{m_1}, τ_{m_2}	Coarse gimbal driving torques
$(\phi_s, \theta_s, \psi_s)$	Components of α_s
ϕ_g	Elevation coarse gimbal angle
$(\phi_p, \theta_p, \psi_p)$	Components of α_p
$(\phi_q, \theta_q, \psi_q)$	Components of α_q
ϕ_1	Target pointing angle
ϕ_{1_g}	Normalized value of ϕ_g
θ_g	Lateral coarse gimbal angle
θ_1	Target pointing angle
θ_{1_g}	Normalized value of θ_g
Ω_{g_1}	Angular velocity of g_1 frame relative to s-frame
Ω_{g_2}	Angular velocity of g_2 frame relative to g_1 frame
ω	Inertial angular velocities, natural frequencies
ζ_{AB}	Position of point A in coordinate system B

Subscripts

i	Inertial frame (X_i, Y_i, Z_i)
i_1	Inertial frame $(X_{i_1}, Y_{i_1}, Z_{i_1})$
g_1	Elevation coarse gimbal
g_2	Lateral coarse gimbal
p	Payload
q	Payload frame (X_q, Y_q, Z_q)
s	Shuttle
o	Norminal or measured parameters

2. SUMMARY OF RESEARCH ACCOMPLISHMENTS

2.1 Research Accomplishments

The system configuration considered in this study is shown in figure 3. A detailed mathematical model of the space shuttle/coarse gimbals/fine pointing system was developed using the Lagrangian approach. The model automatically includes all the internal couplings. The equations were linearized around a set of target angles in order to maintain the mathematical tractability of the problem, and to facilitate the derivation of appropriate control laws. Control systems were designed for the elevation and lateral coarse gimbals, which minimize the sum of the norms of the 3-dimensional centering errors at the four-bearing stations. Thus the coarse gimbals automatically and continuously follow the payload in the solar-, stellar-, Earth-pointing modes. Control laws were designed for the magnetic suspension and fine pointing actuators, which minimize the sum of the norms of the 3-dimensional magnetic forces at each bearing station. The canonical mathematical model for the space shuttle/ASP system has 11 degrees of freedom (order 22). Sensor noise and actuator noise are also included in the model. This model, when coupled with the crew-motion model (ref. 2) of order 24, results in the total system order of 46. A computer program has been prepared to generate the system matrixes, and to solve the the resulting covariance equation.

2.2 Planned Publications

A paper on the mathematical model of the Annular Suspension and Pointing System and Predicted Performance Under Stochastic Crew Motion Disturbances and Sensor Noise is being planned, for submission probably to the AIAA Journal of Spacecraft and Rockets. This paper shall include forthcoming numerical results.

3. MATHEMATICAL MODEL DEVELOPMENT

3.1 Mathematical Model Development

(X_i, Y_i, Z_i) is an inertial system centered at O_i. (X_s, Y_s, Z_s) is a shuttle-fixed system, centered at O_s, the shuttle center of mass (fig. 3). O_s nominally coincides with O_i. $(X_{g_1}, Y_{g_1}, Z_{g_1})$ is a coordinate system

fixed to the elevation coarse gimbal, centered at P_1, and is obtained by one rotation ϕ_g about X_{g_1}. The axis X_{g_1} remains parallel to X_s. The coordinate system $(X_{g_2}, Y_{g_2}, Z_{g_2})$ is fixed to the lateral coarse gimbal. This system is centered at P_2, and is obtained from the g_1 system by one rotation θ_g about Y_{g_2}. All the coordinate systems will hereafter be referred to by their subscripts, e.g. i, s, g_1, g_2, etc.

Another inertial coordinate system $(X_{i_1}, Y_{i_1}, Z_{i_1})$ is also centered at O_i, and is obtained by two rotations ϕ_1, θ_1 (X, Y sequence) from the i-system. ϕ_1 and θ_1 represent the target pointing angles relative to the i-frame.

The payload assembly consists of a cylindrical payload instrument, the instrument mounting surface, and the annular rim (fig. 4). (X_p, Y_p, Z_p) is a coordinate system fixed to the payload assembly, centered at O, its center of mass. The payload-fixed coordinate system (X_q, Y_q, Z_q) is parallel to (X_p, Y_p, Z_p), and is centered at point Q, which is the center of the instrument mounting surface.

The coordinate system (X_s, Y_s, Z_s) is obtained from (X_i, Y_i, Z_i) by a set of three rotations ϕ_s, θ_s, ψ_s in X, Y, Z sequence. The vector $\alpha_s = (\phi_s, \theta_s, \psi_s)^T$ thus defines the shuttle attitude. The payload system (X_p, Y_p, Z_p) is obtained from the i_1 system by a set of three rotations (X, Y, Z sequence) ϕ_p, θ_p, ψ_p. Thus the vector $\alpha_p = (\phi_p, \theta_p, \psi_p)^T$ defines the payload attitude.

In the material that follows, ζ_{AB} denotes the coordinates of point A in the B coordinate system; v_{ABC} denotes the linear velocity of point A relative to the B-frame, expressed along the C-coordinates. The vector ω denotes the inertial angular velocity of the body expressed along the body-coordinates, while Ω denotes relative angular velocity vector (as given in the list of symbols). The matrix D_{AB} denotes the transformation matrix from A-coordinate system to B-coordinate system.

3.2 Summary of Mathematical Model

The mathematical model is obtained via Lagrangian formulation. The complete system consists of two separate systems: i) shuttle and coarse gimbals, and ii) payload assembly. Since these two systems are physically separated by magnetic actuator gaps, it was advantageous to derive separate models for each system, and to interconnect them via magnetic actuator forces.

The coarse pointing assembly consists of three objects; shuttle, elevation gimbal, and lateral gimbal. Expressions are derived for the kinetic energies of the three objects in terms of the inertial velocities of their centers of mass, and their angular velocities relative to the inertial frame, expressed along the body coordinates of each object. The eight degrees of freedom are:

$$\zeta_{O_s ii} = (X_{O_s i}, Y_{O_s i}, Z_{O_s i})^T, \quad \alpha_s, \quad \phi_g \quad \text{and} \quad \theta_g.$$

The gimbal bearings are assumed to be frictionless. For the payload assembly, the six degrees of freedom are:

$$\alpha_p \quad \text{and} \quad \zeta_{Oi_1} = (X_{Oi_1}, Y_{Oi_1}, Z_{Oi_1})^T.$$

Linearization is performed about:

$$\zeta_{O_s i} \equiv 0, \quad \alpha_s \equiv 0, \quad \phi_g \equiv \phi_1, \quad \theta_g \equiv \theta_1, \quad \alpha_p \equiv 0,$$

$$\zeta_{Oi_1} \equiv \zeta_{Oi_1} \quad \text{(nominal)}.$$

Total degrees of freedom are 14; however, since only the relative position of the payload assembly, relative to the coarse pointing assembly is of interest, three degrees of freedom are redundant. Thus there are eleven minimal degrees of freedom.

3.3 Kinetic Energy of the Shuttle

The inertial angular velocity of the shuttle resolved along the s-system is

$$\omega_s = E_s \dot{\alpha}_s \tag{1}$$

where

$$E_s = \begin{bmatrix} \cos\theta_s \cos\psi_s & \sin\psi_s & 0 \\ -\cos\theta_s \sin\psi_s & \cos\psi_s & 0 \\ \sin\theta_s & 0 & 1 \end{bmatrix} \tag{2}$$

The linear velocity of O_s in the i-frame, expressed along i-frame is

$$v_{O_s ii} = \dot{\zeta}_{O_s i}.$$

The kinetic energy of the shuttle is given by:

$$T_s = \frac{1}{2} m_s v^T_{O_s ii} v_{O_s ii} + \frac{1}{2} \dot{\alpha}_s^T E_s^T I_s E_s \dot{\alpha}_s \tag{3}$$

where

$$I_s = \begin{bmatrix} I_{XX_s} & -I_{XY_s} & -I_{XZ_s} \\ -I_{XY_s} & I_{YY_s} & -I_{YZ_s} \\ -I_{XZ_s} & -I_{YZ_s} & I_{ZZ_s} \end{bmatrix} \tag{4}$$

3.4 Kinetic Energy of the Elevation Coarse Gimbal

The inertial angular velocity of the gimbal g_1 resolved along g_1 frame is

$$\omega_g = \Omega_{g_1} + D_{sg_1}\, \omega_s \tag{5}$$

where

$$\Omega_{g_1} = (\dot{\phi}_g,\ 0,\ 0)^T \qquad D_{sg_1} = T_1\ (\phi_g)$$

(Ω_{g_1} = angular velocity of elevation coarse gimbal w. r. t. the shuttle)

The linear inertial velocity of the center of mass (located at P_1) expressed along i-coordinates is

$$v_{P_1 ii} = v_{O_s ii} + D_{is}^T \left[\omega_s \times \zeta_{p_1 s}\right] \tag{6}$$

$$= v_{O_s ii} + D_{is}^T H_{P_1} E_s\, \dot{\alpha}_s \tag{7}$$

where

$$H_{p_1} = -C_p\ (\zeta_{p_1 s}) \tag{8}$$

Kinetic energy

$$T_{g_1} = \frac{1}{2}\, m_{g_1}\, v_{P_1 ii}^T\, v_{p_1 ii} + \frac{1}{2}\, \omega_{g_1}^T\, I_{g_1}\, \omega_{g_1} \tag{9}$$

where I_{g_1} is defined similar to (4).

3.5 Kinetic Energy of the Lateral Coarse Gimbal

The inertial angular velocity of lateral gimbal resolved along the g_2-axes is

$$\omega_{g_2} = \Omega_{g_2} + D_{g_1 g_2}\, \omega_{g_1}$$

or

$$\omega_{g_2} = \Omega_{g_2} + D_{g_1 g_2}\, \Omega_{g_1} + D_{g_1 g_2}\, D_{sg_1}\, \omega_s \tag{10}$$

where

$\Omega_{g_2} = (0, \dot{\theta}_g, 0)^T$ = angular velocity of lateral gimbal (along g_2 coordinates) relative to g_1 frame.

The linear velocity of the center of mass (P_2) relative to s-frame resolved along g_1 is

$$v_{P_2 s g_1} = v_{P_1 s g_1} + \Omega_{g_1} \times \zeta_{P_2 g_1} + v_{P_2 g_1 g_1}$$

But

$$v_{P_2 s s} = D^T_{s g_1} v_{P_2 s g_1},$$

and

$$v_{P_2 i s} = v_{O_s i s} + v_{P_2 s s} + \omega_s \times \zeta_{P_2 s}$$

therefore

$$v_{P_2 i s} = v_{O_s i s} + D_{s g_1}^T (v_{P_1 s g_1} + \Omega_{g_1} \times \zeta_{P_2 g_1}) + \omega_s \times (\zeta_{P_1 s} + D_s^T{}_{g_1} \zeta_{P_2 g_1})$$

Point P_1 is fixed relative to the shuttle;

$$v_{P_1 s g_1} = 0.$$

Since

$$\zeta_{P_2 g_1} = (0, 0, z_{P_2 g_1})^T,$$

after simplification,

$$v_{P_2 i s} = D_{is} v_{O_s i i} + \dot{\gamma} + H_{P_2 s} E_s \dot{\alpha}_s \tag{11}$$

where

$$\gamma = (0, -\sin \phi_g, \cos \phi_g)^T z_{P_2 g_1} \tag{12}$$

$$H_{P_2 s} = -C_p (\zeta_{P_1 s} + \gamma) \tag{13}$$

Kinetic energy

$$T_{g_2} = \frac{1}{2} m_{g_2} v_{P_2}^T{}_{is} v_{P_2 i s} + \frac{1}{2} \omega_{g_2}^T I_{g_2} \omega_{g_2} \tag{14}$$

3.6 Kinetic Energy of Payload Assembly

For the payload assembly, it was found to be advantageous to use the coordinate system (X_q, Y_q, Z_q) for obtaining the equations of motion. The (X_q, Y_q, Z_q) system, which is payload fixed, is obtained from the i_1-system

via three rotations $(\phi_q, \theta_q, \psi_q) = \alpha_q^T$ in 1, 2, 3, sequence, and by translating the origin to Q which is the center of the instrument mounting surface. The vector α_q then defines the payload attitude. The payload angular velocity relative to the inertial frame, resolved along the q-axes, is

$$\omega_q = E_q \dot{\alpha}_q \tag{15}$$

where E_q is defined in a manner similar to E_s (equation 2).

The kinetic energy is given by

$$T_p = \frac{1}{2} m_p v_Q^T{}_{iq} v_{Qiq} + \frac{1}{2} \omega_q^T I_q \omega_q + m_p \left[v_Q^T{}_{iq} H_{oq} \omega_q \right] \tag{16}$$

where

$$H_{oq} = -C_p(\zeta_{oq}) \tag{17}$$

and I_q = inertia matrix of the payload assembly about the q-axes.

3.7 Generalized Forces

The generalized forces are obtained by increasing one generalized coordinate at a time, from q_r to $q_r + \delta_{qr}$, all other coordinates being fixed, and by examining the expressions for work done. Thus the generalized forces for the generalized coordinates are as follows:

Coordinate(s)	Generalized force
$\zeta_{O_s i}$	$F_c - D_{sg_1}^T D_{g_1 g_2}^T \sum_{j=1}^{4} F_j$
α_s	$T_c + T_{con} - \begin{bmatrix} \tau_{m_1} \\ 0 \\ 0 \end{bmatrix} - D_{s g_1}^T \begin{bmatrix} 0 \\ \tau_{m_2} \\ 0 \end{bmatrix} - \sum_{j=1}^{4} \zeta_{Bjs} \times (D_{s g_1}^T D_{g_1 g_2}^T F_j) + \zeta_c \times F_c$
ϕ_g	$\tau_{m_1} - e_1^T \sum_{j=1}^{4} \zeta_{Bjg_1} \times (D_{g_1 g_2}^T F_j)$
θ_g	$\tau_{m_2} - e_2^T \sum_{j=1}^{4} \zeta_{Bjg_2} \times F_j$
ζ_{Qi_1}	$\sum_{j=1}^{4} F_j$
α_q	$\sum_{j=1}^{4} \zeta_{Ajq} \times F_j$

(ζ_c = crew location in the s-system)

3.8 Equations of Motion

The total kinetic energy of the shuttle and the coarse pointing assembly is

$$
\begin{aligned}
T &= T_s + T_{g1} + T_{g2} \\
&= \tfrac{1}{2} m_s \dot{\zeta}_{O_s i}^T \dot{\zeta}_{O_s i} + \tfrac{1}{2} \dot{\alpha}_s^T E_s^T I_s E_s \dot{\alpha}_s \\
&\quad + \tfrac{1}{2} m_{g1} (\dot{\zeta}_{O_{si}} + D_{is}^T H_{p1} E_s \dot{\alpha}_s)^T (\dot{\zeta}_{O_{si}} + D_i^T{}_s H_{p1} E_s \dot{\alpha}_s) \\
&\quad + \tfrac{1}{2} (\Omega_{g1} + D_{sg1} E_s \dot{\alpha}_s)^T I_{g1} (\Omega_{g1} + D_{sg1} E_s \dot{\alpha}_s) \\
&\quad + \tfrac{1}{2} m_{g2} (D_{is} \dot{\zeta}_{O_s i} + \dot{\gamma} + H_{p2s} E_s \dot{\alpha}_s)^T (D_{is} \dot{\zeta}_{O_s i} + \dot{\gamma} + H_{p2s} E_s \dot{\alpha}_s) \\
&\quad + \tfrac{1}{2} (\Omega_{g2} + D_{g1g2} \Omega_{g1} + D_{g1g2} D_{sg1} \omega_s)^T I_{g2} (\Omega_{g2} + D_{g1g2} \Omega_{g1} \\
&\qquad + D_{g1g2} D_{sg1} \omega_s) \qquad (18)
\end{aligned}
$$

The equations of motion are given by:

$$
\frac{d}{dt}\left(\frac{\partial T}{\partial \dot{q}_r}\right) - \frac{\partial T}{\partial q_r} = F_{q_r} \qquad (19)
$$

where q_r, r=1, 2, ..., n, are the generalized coordinates and F_{q_r} are the generalized forces. Application of (19) to the kinetic energy in equation (18) results in the equations of motion, which are nonlinear and highly complex. Linearization is performed about the equilibrium point.

$$
\zeta_{O_s i} \equiv 0, \quad \alpha_s \equiv 0, \quad \phi_g \equiv \phi_1, \quad \theta_g \equiv \theta_1
$$

and the following equations are obtained:

$$
m\ddot{\zeta}_{O_s i} + (m_{g1} H_{p1} + m_{g2} H_{p2s}) \ddot{\alpha}_s + hz_{p2g1} m_{g2} \ddot{\phi}_g = F_{\zeta O_s i} \qquad (20)
$$

where

$$
m = m_s + m_{g1} + m_{g2}
$$

$$(I_s + m_{g_1} H_{p_1}^T H_{p_1} + m_{g_2} H_{p_2}^T{}_s H_{p_2 s} + D_s^T{}_{g_1} I_{g_1} D_{sg_1} + D_{ii_1}^T I_{g_2} D_{ii_1}) \ddot{\alpha}_s$$
$$+ (m_{g_1} H_{p_1}^T + m_{g_2} H_{p_2}^T{}_s) \ddot{\zeta}_{O_s i} + D_s^T{}_{g_1} I_{g_1} e_1 + m_{g_2} z_{p_2 g_1} H_{p_2}^T{}_s h$$
$$+ D_i^T{}_{i_1} I_{g_2} D_{g_1 g_2} e_1) \ddot{\phi}_g + D_i^T{}_{i_1} I_{g_2} e_2 \ddot{\theta}_g = F_{\alpha_s} \quad (21)$$

$$(m_{g_2} z_{p_2 g_1} h^T) \ddot{\zeta}_{O_s i} + (e_1^T I_{g_1} D_{sg_1} + z_{p_2 g_1} h^T H_{p_2 s} m_{g_2}$$
$$+ e_1^T D_{g_1 g_2}^T I_{g_2} D_{ii_1}) \ddot{\alpha}_s + (I_{XXg_1} + e_1^T D_{g_1 g_2}^T I_{g_2} D_{g_1 g_2} e_1$$
$$+ m_{g_2} z_{p_2 g_1}^2) \ddot{\phi}_g + e_2^T I_{g_2} D_{g_1 g_2} e_1 \ddot{\theta}_g = F_{\phi g} \quad (22)$$

$$I_{YYg_2} \ddot{\theta}_g + e_2^T I_{g_2} D_{g_1 g_2} e_1 \ddot{\phi}_g + e_2^T I_{g_2} D_{g_1 g_2} D_{sg_1} \ddot{\alpha}_s = F\theta_g \quad (23)$$

In equations (21) - (23), the symbols $\zeta_{O_s i}$, α_s, ϕ_g, θ_g denote their incremental values about the equilibrium point. D_{sg_1}, $D_{g_1 g_2}$ denote the corresponding transformation matrices evaluated at constant angles ϕ_1 and θ_1, and $D_{ii_1} = D_{g_1 g_2} D_{sg_1}$ (evaluated at ϕ_1, θ_1).

For the payload assembly, the linearized equations around

$$\alpha_q \equiv 0, \quad \zeta_{Qi_1} \equiv 0$$

are:

$$m_p (\ddot{\zeta}_{Qi_1} + H_{oq} \ddot{\alpha}_q) = F_{\zeta Qi_1} \quad (24)$$

$$I_q \ddot{\alpha}_q + m_p H_{oq}^T \ddot{\zeta}_{Qi_1} = F_{\alpha q} \quad (25)$$

substituting for $\ddot{\zeta}_{Qi}$ from (24) into (25),

$$(I_q - m_p H_{oq}^T H_{oq}) \ddot{\alpha}_q = F_{\alpha q} - H_{oq}^T F_{\zeta Qi_1} \quad (26)$$

But the moment of inertia of the payload assembly about the p-axes is

$$I_p = I_q - m_p H_{oq}^T H_{oq}.$$

Also, for the linearized system,

$$\alpha_q = \alpha_p$$

Therefore, equation (26) becomes:

$$I_p \ddot{\alpha}_p = F_{\alpha q} - H_{oq}^T F_{\zeta Qi_1} \quad (27)$$

Considering the two position equations, (20) for $\zeta_{O_s i}$, and (24) for ζ_{Qi_1}, only the difference between the payload assembly position and the coarse pointing assembly is of interest.

Define

$$\varepsilon = \zeta_{p_2 i_1} - \zeta_{Qi_1} \tag{28}$$

Before linearization,

$$\zeta_{p_2 i_1} = D_{ii_1}\, r_{O_s i} + D_{ii_1}\, D_i^T{}_s\, D_s^T{}_{g_1}\, \zeta_{p_2 g_1} + D_{ii_1}\, D_i^T{}_s\, \zeta_{p_1 s}$$

After linearization of the second derivatives of this equation about the equilibrium point, simplification yields

$$\ddot{\zeta}_{O_s i} = D_i^T{}_{i_1}\,(\ddot{\varepsilon} + \ddot{\zeta}_{Qi_1}) - H_{p_2 s}\,\ddot{\alpha}_s - hz_{p_2 g_1}\,\ddot{\phi}_g \tag{29}$$

This value of $\ddot{\zeta}_{O_s i}$ is substituted into equations (20) - (23) to obtain the following:

$$\ddot{\varepsilon} + D_{ii_1}\left(\frac{m_{g_1}}{m} H_{p_1} - \frac{m_s + m_{g_1}}{m} H_{p_2 s}\right)\ddot{\alpha}_s$$

$$-D_{ii_1}\left(\frac{m_s + m_{g_1}}{m}\right) hz_{p_2 g_1}\,\ddot{\phi}_g - H_{oq}\,\ddot{\alpha}_q = \frac{D_{ii_1}}{m} F_c$$

$$-\left(\frac{1}{m} + \frac{1}{m_p}\right)\sum_{i=1}^{4} F_i \tag{30}$$

where F_c is the crew-motion force. The remaining equations of motion are:

$$(I_s + m_{g_1} H_{p_1}^T H_{p_1} - m_{g_1} H_{p_1}^T H_{p_2 s} + D_{sg_1}^T I_{g_1} D_{sg_1} + D_i^T{}_{i_1} I_{g_2} D_{ii_1})\ddot{\alpha}_s$$

$$+ (m_{g_1} H_{p_1}^T + m_{g_2} H_{p_2}^T{}_s)\, D_i^T{}_{i_1}\,\ddot{\varepsilon} + (D_s^T{}_{g_1} I_{g_1} e_1$$

$$+ D_i^T{}_{i_1} I_{g_2} D_{g_1 g_2} e_1 - m_{g_1} H_{p_1}^T hz_{p_2 g_1})\,\ddot{\phi}_g + D_i^T{}_{i_1} I_{g_2} e_2\,\ddot{\theta}_g$$

$$- (m_{g_1} H_{p_1}^T + m_{g_2} H_{p_2 s}^T)\, D_i^T{}_{i_1} H_{oq}\,\ddot{\alpha}_p = T_c + T_{con}$$

$$-\begin{pmatrix} \tau_{m_1} \\ \tau_{m_2} \cos\phi_1 \\ \tau_{m_2} \sin\phi_1 \end{pmatrix} - \sum_{j=1}^{4} C_p\,(\zeta_{Bjs})\left(D_i^T{}_{i_1} F_j\right)$$

$$- \frac{(m_{g_1} H_{p_1}^T + m_{g_2} H_{p_2}^T s)}{m_p} D_{i\,i_1}^T \sum_{j=1}^{4} F_j + \zeta_c \times F_c \qquad (31)$$

$$m_{g_2} z_{p_2 g_1} h^T D_{i\,i_1}^T \ddot{\varepsilon} + (e_1^T I_{g_1} D_{s g_1} + e_1^T D_{g_1 g_2}^T I_{g_2} D_{i i_1}) \ddot{\alpha}_s$$
$$+ (I_{XX g_1} + e_1^T D_{g_1 g_2}^T I_{g_2} D_{g_1 g_2} e_1) \ddot{\phi}_g$$
$$+ e_2^T I_{g_2} D_{g_1 g_2} e_1 \ddot{\theta}_g - m_{g_2} z_{p_2 g_1} h^T D_{i\,i_1}^T H_{oq} \ddot{\alpha}_p$$
$$= \tau_{m_1} - e_1^T \sum_{j=1}^{4} C_p (\zeta_{B j g_1}) D_{g_1 g_2}^T F_j$$

$$- \frac{m_{g_2}}{m_p} z_{p_2 g_1} h^T D_{i\,i_1}^T \sum_{j=1}^{4} F_j \qquad (32)$$

$$I_{YY g_2} \ddot{\theta}_g + e_2^T I_{g_2} D_{g_1 g_2} e_1 \ddot{\phi}_g + e_2^T I_{g_2} D_{i i_1} \ddot{\alpha}_s$$
$$= \tau_{m_2} - e_2^T \sum_{j=1}^{4} C_p (\zeta_{B j g_2}) F_j \qquad (33)$$

$$I_p \ddot{\alpha}_p = \sum_{j=1}^{4} C_p (\zeta_{A jq} - \zeta_{oq}) F_j \qquad (34)$$

Equations (30) - (34) define the complete linearized motion of the system.

Position Sensor Outputs:

An axial and a radial position sensor is located at each magnetic actuator station. For computing the magnetic actuator forces, it is necessary to compute the centering errors at each actuator station. Since the payload assembly rim is continuous, it is necessary to compute the points on the rim directly under the actuator stations. This can be done by minimizing over rim roll angle ψ, the distance between a point on the rim (assumed to be a circle) and a magnetic actuator station. For the present linear analysis, however, this can be achieved by a simpler method. The linearized radial centering errors are simply the radial components of ε. The axial centering errors are obtained by finding the angle between the bearing plane and the rim plane. The vector $\zeta_{B j g_2}$ is transformed ("projected") into the q´- coordinate system (with $\varepsilon = 0$), q´- system being same as the q-system, but without the ψ_p = rotation. The Z-component of the transformed vector $\zeta_{B jq'}$, plus the axial (Z-axis) components of translation error ε, gives the total axial centering errors. Let $\delta_j(x)$ denote the X_{g_2}-axis centering error at the jth actuator station, etc.

First ignoring the translation,

$$\zeta_{Bjq'} = T_2(\theta_p)\ T_1(\phi_p)\ D_{ii_1}\ D_{is}^T\ D_{sg_1}^T\ D_{g_1g_2}^T\ \zeta_{Bjg_2} \tag{35}$$

After linearization and simplification, the following expressions for the sensor outputs are obtained:

$$\delta_1(x) = \delta_3(x) = \epsilon_x \tag{36}$$

$$\delta_2(y) = \delta_4(y) = \epsilon_y \tag{37}$$

$$\delta_1(z) = \epsilon_z - r(\cos\phi_1\ \theta_s + \sin\phi_1\ \psi_s) - r(\theta_g - \theta_p) \tag{38}$$

$$\delta_2(z) = \epsilon_z + r(\cos\theta_1\ \phi_s + \sin\theta_1 \sin\phi_1\ \theta_s - \sin\theta_1 \cos\phi_1\ \psi_s) + r(\phi_g \cos\theta_1 - \phi_p) \tag{39}$$

$\delta_3(z)$ and $\delta_4(z)$ are obtained from $\delta_1(z)$ and $\delta_2(z)$ by changing the sign of r.

4. CONTROL SYSTEMS DESIGN

4.1 Coarse Gimbal Control Systems

The coarse gimbal assembly, which consists of the elevation and lateral coarse gimbals, must automatically follow the payload assembly. This is accomplished by the use of two brushless DC torquers. The objective of the control systems for the torquers is to move the coarse gimbals in such a manner that the payload assembly is kept properly centered in the magnetic bearings. Thus an appropriate design approach is to obtain the command values of ϕ_g and θ_g which will minimize

$$J = \delta_1^2(x) + \delta_3^2(x) + \delta_2^2(y) + \delta_4^2(y) + \sum_{j=1}^{4} \delta_j^2(z) \tag{40}$$

This is done by substituting for δ_j from equations (36) to (39), and for ϵ from linearized version of equation (28), and making

$$\frac{\partial J}{\partial \phi_g} = \frac{\partial J}{\partial \theta_g} = 0$$

The solution gives the following command signals:

$$\phi_{gc} - \phi_g = \frac{1}{z^2_{P_2 g_1} + r^2 \cos^2 \theta_1} \left[z_{P_2 g_1} \varepsilon_y - r^2 \cos \theta_1 (\cos \theta_1 \phi_g - \phi_p) \right.$$

$$\left. - r^2 \cos \theta_1 (\cos \theta_1 \phi_s + \sin \theta_1 \sin \phi_1 \theta_s - \sin \theta_1 \cos \phi_1 \psi_s) \right] \quad (41a)$$

$$\theta_{gc} = \theta_p - (\cos \phi_1 \theta_s + \sin \phi_1 \psi_s) \quad (41b)$$

It can also be proved that

$$\phi_{gc} - \phi_g = \frac{1}{z^2_{P_2 g_1} + r^2 \cos^2 \theta_1} \left[z_{P_2 g_1} \delta_2 (y) - \frac{r \cos \theta_1}{2} \right.$$

$$\left. \{\delta_2 (z) - \delta_4 (z)\} \right] \quad (42)$$

and

$$\theta_{gc} - \theta_g = \frac{\delta_1 (z) - \delta_3 (z)}{2r} \quad (43)$$

Equations (41a), (41b) are used for solution of the state equations, and (42), (43) are used in actual implementation.

The torques to be generated by the coarse gimbal torquers are then given by

$$\tau_{m_1} = - K_{g_1} \dot{\phi}_g + L_{g_1} (\phi_{gc} - \phi_g) \quad (44)$$

$$\tau_{m_2} = - K_{g_2} \dot{\theta}_g + L_{g_2} (\theta_{gc} - \theta_g) \quad (45)$$

where K_{g_1}, K_{g_2} are rate gains and L_{g_1}, L_{g_2} are proportional gains. The desired response can be (approximately) obtained by making

$$\frac{K_{g_1}}{I_{XXg_1} + e_1^T D^T_{g_1 g_2} I_{g_2} D_{g_1 g_2} e_1} = 2\rho_{g_1} \omega_{g_1}$$

$$\frac{L_{g_1}}{I_{XXg_1} + e_1^T D^T_{g_1 g_2} I_{g_2} D_{g_1 g_2} e_1} = \omega_{g_1}^2 \quad (46)$$

$$\frac{K_{g_2}}{I_{YYg_2}} = 2\rho_{g_2} \omega_{g_2}, \text{ and } \frac{L_{g_2}}{I_{YYg_2}} = \omega_{g_2}^2 \quad (47)$$

4.2 Magnetic Actuator Control Systems

Magnetic forces acting in X_q, Y_q and Z_q directions (nominal) at each of the four bearing stations are used for controlling the motion of the payload assembly. Thus there are twelve control forces. Ignoring the rotation-translation coupling, the desired responses are obtained by making

$$\begin{bmatrix} \sum_{j=1}^{4} F_{xj} \\ \sum_{j=1}^{4} F_{yj} \\ \sum_{j=1}^{4} F_{zj} \end{bmatrix} = m_{10}\, \lambda_{\varepsilon}$$

and

$$C_{\zeta o} \sum_{j=1}^{4} F_j - rf = -I_{po}\, \lambda_{\alpha p}$$

where

$$f = (F_{z_4} - F_{z_2},\ F_{z_1} - F_{z_3},\ F_{x_2} - F_{x_4} + F_{y_3} - F_{y_1})^T$$

$$m_1 = mm_p/(m + m_p),\ C_{\zeta} = -C_p\ (\zeta_{oq}),\ \lambda_{\varepsilon} = (\lambda_{\varepsilon x},\ \lambda_{\varepsilon y},\ \lambda_{\varepsilon z})^T$$

$$\lambda_{\varepsilon x} = 2\rho_x\, \omega_x\, \dot{\varepsilon}_x + \omega_x^2\, \varepsilon_x, \text{ etc.}$$

The subscript "o" implies the measured or estimated value of the parameter. Thus the control force equation can be written in the following matrix-vector form:

$$A_{CF}\, F = q$$

where

$$F = (F_{x_1},\ F_{x_2},\ F_{x_3},\ F_{x_4},\ F_{y_1},\ F_{y_2},\ F_{y_3},\ F_{y_4},\ F_{z_1},\ F_{z_2},\ F_{z_3},\ F_{z_4})^T$$

$$q = \left[m_{10}\, \lambda_{\varepsilon}^T,\ \frac{1}{r}\, (I_{po}\, \lambda_{\alpha p} + C_{\zeta o}\, m_{10}\, \lambda_{\varepsilon})^T \right]^T \tag{48}$$

A_{CF} = appropriate 6 × 12 coefficient matrix.

Letting

$$\left.\begin{aligned} F_{x_1} = F_{x_3} &= \tfrac{1}{2}\, m_{10}\, e_1^T\, \lambda_{\varepsilon} \\ F_{y_2} = F_{y_4} &= \tfrac{1}{2}\, m_{10}\, e_2^T\, \lambda_{\varepsilon} \end{aligned}\right\} \tag{49}$$

The remaining equations are:

$$A'_{CF}\, F' = q',$$

or

$$\begin{bmatrix} 1 & 1 & 0 & 0 & 0 & 0 & 0 & 0 \\ 0 & 0 & 1 & 1 & 0 & 0 & 0 & 0 \\ 0 & 0 & 0 & 0 & 1 & 1 & 1 & 1 \\ 0 & 0 & 0 & 0 & 0 & -1 & 0 & 1 \\ 0 & 0 & 0 & 0 & 1 & 0 & -1 & 0 \\ 1 & -1 & -1 & 1 & 0 & 0 & 0 & 0 \end{bmatrix} \begin{bmatrix} F_{x_2} \\ F_{x_4} \\ F_{y_1} \\ F_{y_3} \\ F_{z_1} \\ F_{z_2} \\ F_{z_3} \\ F_{z_4} \end{bmatrix} = q - \begin{bmatrix} F_{x_1} + F_{x_3} \\ F_{y_2} + F_{y_4} \\ 0 \\ 0 \\ 0 \\ 0 \end{bmatrix}$$

The solution which minimizes the norm of F' is given by

$$F' = (A'_{CF})^T \left\{ A'_{CF}\, (A'_{CF})^T \right\}^{-1} q'$$

which, after simplification, gives:

$$F_{x_2} = \frac{1}{4r}\, r\, e_3^T\, (I_{po}\, \lambda_{\alpha p} + C_{\zeta o}\, m_{10}\, \lambda_\varepsilon) \tag{50}$$

$$F_{x_4} = -F_{x_2} \tag{51}$$

$$F_{y_1} = F_{x_4} \tag{52}$$

$$F_{y_3} = F_{x_2} \tag{53}$$

$$F_{z_1} = \frac{1}{4}\, m_{10}\, e_3^T\, \lambda_\varepsilon + \frac{1}{2r}\, e_2^T\, (I_{po}\, \lambda_{\alpha p} + C_{\zeta o}\, m_{10}\, \lambda_\varepsilon) \tag{54}$$

$$F_{z_2} = \frac{1}{4}\, m_{10}\, e_3^T\, \lambda_\varepsilon - \frac{1}{2r}\, e_1^T\, (I_{po}\, \lambda_{\alpha p} + C_{\zeta o}\, m_{10}\, \lambda_\varepsilon) \tag{55}$$

$$F_{z_3} = \frac{1}{4}\, m_{10}\, e_3^T\, \lambda_\varepsilon - \frac{1}{2r}\, e_2^T\, (I_{po}\, \lambda_{\alpha p} + C_{\zeta o}\, m_{10}\, \lambda_\varepsilon) \tag{56}$$

$$F_{z_4} = \frac{1}{4}\, m_{10}\, e_3^T\, \lambda_\varepsilon + \frac{1}{2r}\, e_1^T\, (I_{po}\, \lambda_{\alpha p} + C_{\zeta o}\, m_{10}\, \lambda_\varepsilon) \tag{57}$$

This can be expressed as:

$$F = Aq$$

where

$$A^T = \frac{1}{2}\begin{bmatrix} e_1 & o & e_1 & o & o & e_2 & o & e_2 & \frac{1}{2}e_3 & \frac{1}{2}e_3 & \frac{1}{2}e_3 & \frac{1}{2}e_3 \\ o & \frac{1}{2}e_3 & o & -\frac{1}{2}e_3 & -\frac{1}{2}e_3 & o & \frac{1}{2}e_3 & o & e_2 & -e_1 & -e_2 & e_1 \end{bmatrix}$$

Let

$$A_i = \begin{bmatrix} e^T_i \\ e^T_{i+4} \\ e^T_{i+8} \end{bmatrix} \qquad i = 1, 2, 3, 4 \tag{58}$$

Then

$$F_i = A_i\, Aq \qquad i = 1, 2, 3, 4 \tag{59}$$

These are the expressions for desired magnetic actuator forces.

4.3 Space Shuttle Attitude Control System

The attitude of the shuttle is assumed to be controlled by such devices as CMG's or AMCD. The control torque is given by

$$T_{con} = -(I_s + m_{g_1} H_{p_1}{}^T H_{p_1} + m_{g_2} H_{p_2}{}^T{}_s H_{p_2 s})\, \lambda_{\alpha_s} \tag{60}$$

where

$$\lambda_{\alpha_s} = (\lambda_{\phi_s}, \lambda_{\theta_s}, \lambda_{\psi_s})^T \tag{61}$$

$$\lambda_{\phi_s} = 2\rho_{\phi_s}\, \omega_{\phi_s}\, \dot{\phi}_s + \omega^2_{\phi_s}\, \phi_s, \text{ etc.} \tag{62}$$

5. COMPUTATIONAL ASPECTS

5.1 Equations of Motion When Actual Payload Parameters Differ From the Nominal Ones

The control systems designed in the preceeding section are based on nominal or measured values of the parameters ζ_{oq}, m_p and I_p, which are, in general, different from the actual values. It is desirable to investigate the pointing performance when such errors exist. To keep the number of variables small, it is assumed that the same per unit error δ exists between the actual and measured (or nominal) values of these parameters, i.e.

$$C_\zeta = (1 + \delta)\, C_{\zeta o},\ m_p = (1 + \delta)\, m_{po},\ I_p = (1 + \delta)\, I_{po}.$$

Then equation (34) becomes

$$I_p \ddot{\alpha}_p = (C_\zeta - C_{\zeta o})\, m_{10}\, \lambda_\varepsilon - I_{po}\, \lambda_{\alpha p} \tag{63}$$

or

$$(1 + \delta)\, I_{po} \ddot{\alpha}_p = \delta C_{\zeta o}\, m_{10}\, \lambda_\varepsilon - I_{po}\, \lambda_{\alpha p} \tag{64}$$

which reduces to

$$\ddot{\alpha}_p = \frac{\delta}{1+\delta}\, I^{-1}_{po}\, C_{\zeta o}\, m_{10}\, \lambda_\varepsilon - \frac{1}{1+\delta}\, \lambda_{\alpha p} \tag{65}$$

Similarly, equation (30) becomes

$$\ddot{\varepsilon} + A_{12}\, \ddot{\alpha}_s + A_{13}\, \ddot{\phi}_g + A_{15}\, \ddot{\alpha}_p = \frac{D_{ii_1}}{m} F_c - \frac{1}{1+\delta}\left(1 + \frac{\delta m_{po}}{m + m_{po}}\right) \lambda_\varepsilon \tag{66}$$

where A_{12}, A_{13} and A_{14} are easily identified by examining equation (30).

In an attempt to normalize the equations of motion to some extent, the Euclidian norm $\|\zeta_{oqo}\|$, hereafter denoted by $\|\zeta\|$, was selected as the normalizing parameter. The following variables and parameters are defined:

$$E_o = m_{10}\, I_{po}^{-1}\, \|\zeta\|^2,\ C_1 = C_{\zeta o}/\|\zeta\|,\ \nu = \varepsilon/\|\zeta\|,\ \beta_s = \alpha_s/\|\zeta\|,$$

$$\phi_{1g} = \phi_g/\|\zeta\|,\ \theta_{1g} = \theta_g/\|\zeta\|,\ f_c = F_c/\|\zeta\|,\ t_c = T_c/\|\zeta\|$$

The normalized equations of motion then become

$$\ddot{\nu} + A_{12}\, \ddot{\beta}_s + A_{13}\, \ddot{\phi}_{1g} + A_{15}\, \ddot{\alpha}_p = B_{11}\, f_c - \frac{1}{1+\delta}\left(1 + \delta \frac{m_{po}}{m + m_{po}}\right) \lambda_\nu \tag{67}$$

$$A_{21}\, \ddot{\nu} + A_{22}\, \ddot{\beta}_s + A_{23}\, \ddot{\phi}_{1g} + A_{24}\, \ddot{\theta}_{1g} + A_{25}\, \ddot{\alpha}_p = \frac{1}{\|\zeta\|} T_{con} + t_c - \frac{1}{\|\zeta\|} \begin{bmatrix} \tau_{m_1} \\ \tau_{m_2} \cos\phi_1 \\ \tau_{m_2} \sin\phi_1 \end{bmatrix} - \sum_{j=1}^{4} C_p\, (\zeta_{Bjs})\, D_i^T{}_i\, F_j$$

$$- \frac{(m_{g_1} H_{p_1}^T + m_{g_2} H_{p_2}^T s)\, D_i^T{}_{\cdot 1}}{(1+\delta)\, m_{po}\, \|\zeta\|} \sum_{j=1}^{4} F_j + \zeta_c \times f_c \tag{68}$$

$$A_{31}\, \ddot{\nu} + A_{32}\, \ddot{\beta}_s + A_{33}\, \ddot{\phi}_{1g} + A_{34}\, \ddot{\theta}_{1g} + A_{35}\, \ddot{\alpha}_p$$

$$= \frac{1}{\|\zeta\|}\left[\tau_{m_1} - e_1^T \sum_{j=1}^{4} C_p\,(\zeta_{Bjg_1})\, D^T_{g_1g_2}\, F_j - \frac{m_{g_2}}{(1+\delta)\, m_{po}}\right.$$

$$\left. z_{p_2g_1} h^T D_{ii_1}{}^T \sum_{j=1}^{4} F_j\right] \qquad (69)$$

$$A_{42}\,\ddot{\beta}_s + A_{43}\,\ddot{\phi}_{1g} + A_{44}\,\ddot{\theta}_{1g} = \frac{1}{\|\zeta\|}\,\tau_{m_2} - \frac{e_2^T}{\|\zeta\|}\sum_{j=1}^{4} C_p\,(\zeta_{Bjg_2})\,F_j \qquad (70)$$

The matrices A_{ij} are given in the appendix.

$$\ddot{\alpha}_p = \frac{\delta}{1+\delta}\,E_o\,C_1\,\lambda_\nu - \frac{1}{1+\delta}\,\lambda_{\alpha p} \qquad (71)$$

Equations (67) - (70) contain the terms $F_j/\|\zeta\|$, $\tau_{mi}/\|\zeta\|$ in their right-hand sides. From equations (59) and (48)

$$\frac{q}{\|\zeta\|} = m_1\,L_1\begin{pmatrix}\lambda_\nu\\ \lambda_{\alpha\rho}\end{pmatrix} \qquad (72)$$

where

$$L_1 = \begin{bmatrix} I_{3\times3} & O_{3\times3} \\ C_1\,\dfrac{\|\zeta\|}{r} & E_o^{-1}\,\dfrac{\|\zeta\|}{r}\end{bmatrix} \qquad (73)$$

Thus the $F_j/\|\zeta\|$ terms in the right-hand rides of equations (67) - (70) can be normalized. The only quantities that remain to be normalized are τ_{m_1} and τ_{m_2}, which are given by equations (44), (45), (41a) and (41b).

After simplification, division by $|\zeta|$ yields

$$\frac{\phi_{gc} - \phi_g}{|\zeta|} = \frac{1}{z^2_{p_2g_1} + r^2\cos^2\theta_1}\left[z_{p_2g_1}\,\nu_y - r^2\cos\theta_1\left\{\left(\cos\theta_1\,\phi_{1g}\right.\right.\right.$$

$$\left.\left.\left. - \frac{\phi_p}{|\zeta|}\right) - (\cos\theta_1,\ \sin\theta_1\sin\phi_1,\ -\sin\theta_1\cos\phi_1)\,\beta_s\right\}\right] \qquad (74)$$

$$\frac{\theta_{gc} - \theta_g}{|\zeta|} = \frac{\theta_p}{|\zeta|} - (0,\ \cos\phi_1,\ \sin\phi_1)\,\beta_s \qquad (75)$$

Hence it is seen that ϕ_{gc} and θ_{gc}, and therefore τ_{m1} and τ_{m2} cannot be normalized in this fashion, and the parameter r or $|\zeta|$ must be specified in addition to the normalized parameters

$$C_1 = C_{\zeta o}/\|\zeta\|,\ r/\|\zeta\|$$

and (76)

$$E_o = m_{10}\,\|\zeta\|^2\, I_{po}^{-1}$$

5.2 Representation of Measurement Noise

Control systems for the coarse gimbals process the measurements of δ_j, j = 1, 2, 3, 4, $\dot{\phi}_g$, $\dot{\theta}_g$, and generate appropriate torque signals. Control systems for magnetic actuators process the measurements of δ_j, j = 1, 2, 3, 4, (for ε and $\dot{\varepsilon}$) and α_p, $\dot{\alpha}_p$ in order to generate appropriate voltages for the magnetic actuator coils (force equations 50 - 57). Space shuttle attitude control system makes use of the shuttle attitude and attitude rate measurements (α_s and $\dot{\alpha}_s$). All these measurements contain certain amounts of noise. The payload assembly attitude α_p and rate $\dot{\alpha}_p$ are estimated by a star-tracker system fixed to the payload which possibly makes use of a Kalman filter. The star-tracker model currently available is discrete-time[3]. However, as a first attempt at the problem, continuous measurements of α_p, $\dot{\alpha}_p$ are assumed to be available, and are represented by adding continuous white noise to the actual quantities. The covariance of the additive noise is to be made equal to that reported in reference 3 using the "optimum system." The results obtained using this approximation are expected to be conservative (showing worse performance than actual) because the actual estimation error is not white, but is band-limited. All other measurements are contaminated with continuous white noise, and appear in all control terms, e.g., λ_ε, $\lambda_{\beta\dot{s}}$, $\lambda_{\alpha p}$, etc. Sensor dynamics have not been included in this first trial, but appropriate representations will be included later. A nonlinear model for the coarse gimbal torquers has been supplied by Sperry Flight Systems, and will be used in task 2, the latter part of the grant. The linear part of this model contains the representation of torque as being proportional to the motor current. Since the control loop contains current feedback, the lag due to inductance can be theoretically made as small as desired. For the second-order model currently available, the eigenvalues represent dynamics which are much faster than the rest of the system; therefore the torque outputs may be assumed to be instantaneous in this first attempt at the solution.

Additive measurement noise contaminates the sensor outputs at the four suspension gaps (δ_j, j = 1, 2, 3, 4), coarse gimbal angle rates, payload attitude and attitude rates. The coarse gimbal angular rates are

measured by tachometers, and the relative displacement rate $(\dot{\varepsilon})$ is generated by using a lead circuit. Thus the measurement noise, represented as white noise processes, appears in all the control terms; e.g., λ_{ν}, $\lambda_{\beta s}$, etc. Each noise term is normalized by division by $\|\zeta\|$.

The crew-motion forces and moments for each crew activity can be described by passing a unity power spectral density white noise through a filter of order four (or less) for each force and each moment.[2] The complete equations of motion can be symbolically written as

$$A \ddot{X}_1 = \bar{A}_1 \dot{X}_1 + \bar{A}_2 X_1 + B_1 f_{cr} + D_1 w_m \tag{77}$$

$$f_{cr} = T X_2 \tag{78}$$

$$\dot{X}_2 = A_2 X_2 + B_2 u$$

where

$$X_1 = (\nu^T, \beta_s{}^T, \phi_{1_g}, \theta_{1_g}, \alpha_p{}^T)^T$$

$$f_{cr} = (f_c{}^T, t_c{}^T)^T \tag{79}$$

X_2 = state vector of crew-motion filters

u = white noise with power spectral density = $1/\|\zeta\|^2$

w_m = measurement noise vector (normalized)

Let

$$X_1 = Y_1$$

$$\dot{X}_1 = Y_2 = \dot{Y}_1$$

$$\dot{Y}_1 = Y_2 \tag{80}$$

$$\dot{Y}_2 = A^{-1} \bar{A}_1 Y_2 + A^{-1} \bar{A}_2 Y_1 + A^{-1} B_1 T X_2 + A^{-1} D_1 w_m \tag{81}$$

$$\dot{X}_2 = A_2 X_2 + B_2 u \tag{82}$$

Thus, defining

$$X = (Y_1{}^T, \dot{Y}_1{}^T, X_2{}^T)^T$$

equations (80), (81) and (82) can be written in the form

$$\dot{X} = \bar{A}\, X + \bar{B}\, \bar{v} \tag{83}$$

where $\bar{v}$ is a vector white noise process.

The resulting covariance equation for this system is

$$\dot{\sum} = \bar{A} \sum + \sum \bar{A}^T + \bar{B}\, \bar{V}\, \bar{B}^T \tag{84}$$

where

$$E\left[\bar{v}\, \bar{v}^T\right] = \bar{V}\, \delta\, (t - \tau) \tag{85}$$

This covariance equation can then be solved for $\sum_{ss}$, the steady state value of $\sum$, by the method described in reference 4.

6.0 PRESENT AND FUTURE EFFORTS

A detailed linearized mathematical model has been derived for the space shuttle/ASP system via Lagrangian formulation. The model incorporates all internal couplings, and sensor noises. The elevation-lateral coarse gimbal configuration has been assumed. Control laws have been designed for the coarse gimbals, which minimize the summed norm of the suspension gap errors at the bearing stations. Thus the coarse gimbals have the capability of automatically and continuously following the payload in order to point at a target which is moving with respect to the space shuttle. Minimum norm control laws have been designed for magnetic suspension and fine-pointing actuators. A computer program has been written for generating the system matrices, and for solving the resulting covariance equation.

In the immediate future, preliminary computational results will be obtained for this model using the program mentioned above. Computation will be performed using data for two or three typical payloads, and statistical pointing accuracies will be obtained as functions of errors in estimating the payload parameters, and sensor noise variances. The star-tracker models which are currently available will be reviewed, and a suitable model will be chosen for inserting in the present mathematical model. (The present mathematical model assumes that the payload attitude estimation error is continuous white noise, with covariance reported in reference 3. This is a conservative assumption and should give worse-than-actual pointing accuracies.) A detailed star-tracker/payload attitude estimator model would be discrete-time; therefore its interconnection with the continuous shuttle/ASPS model will have to be investigated. One solution would be to discretize the continuous system, and

to use equivalent discrete white measurement noises and crew-motion filter input noise. A simpler and computationally less expensive solution would be to approximate the discrete-time star-tracker/estimator system by a continuous system.

The above computational results would also yield the effect of the payload motion on the shuttle. If this is found to be significant, a model for a second payload/ASPS/coarse gimbal system will be added to the present model, and the computation will be repeated. The two payloads are connected only through the shuttle motion; therefore these efforts need be undertaken only if the payload motion is found to significantly affect the shuttle.

If the knowledge of flexible modes of the shuttle is available, this shall be included in the present model as the next step. The linear analysis shall be complete with this step.

The next task is to perform nonlinear analysis. The nonlinearities to be considered include: 1) coarse gimbal torquer nonlinearities due to ripple, cogging and friction; 2) magnetic suspension and fine-pointing actuator nonlinearities: square-law, deadzone, hysteresis, coil switching, etc.; 3) sensor deadzones; and 4) shuttle attitude control system vernier jets, which operate in on-off fashion. The nonlinear system will be represented by a linear part and time-invariant nonlinear blocks. Computational results will be obtained via Monte-Carlo simulations. Finally, time permitting, an analysis of earth-pointing performance shall be performed using the linear model. One way to perform this could be to evaluate the ASP's local pointing performance when tracking a relatively fast-moving target.

APPENDIX

Coefficient Matrices:

$$A_{12} = D_{ii_1}\left(\frac{m_{g_1}}{m} H_{P_1} - \frac{m_s + m_{g_1}}{m} H_{P_2 s}\right)$$

$$A_{13} = - D_{ii_1}\left(\frac{m_s + m_{g_1}}{m}\right) hz_{P_2 g_1}$$

$$A_{15} = - C_1 (1 + \delta)$$

$$B_{11} = \frac{D_{ii_1}}{m}$$

$$A_{21} = \left(m_{g_1} H_{P_1}{}^T + m_{g_2} H_{P_2}{}^T{}_s\right) D^T{}_{ii_1}$$

$$A_{22} = I_s + m_{g_1} H^T{}_{P_1} H_{P_1} - m_{g_1} H^T{}_{P_1} H_{P_2 s} + D^T{}_{sg_1} I_{g_1} D_{sg_1} + D^T{}_{ii_1} I_{g_2} D_{ii_1}$$

$$A_{23} = \left(D^T{}_{sg_1} I_{g_1} + D^T{}_{ii_1} I_{g_2} D_{g_1 g_2}\right) e_1 - m_{g_1} H_{P_1}{}^T hz_{P_2 g_1}$$

$$A_{24} = D^T{}_{ii_1} I_{g_2} e_2$$

$$A_{25} = - \left(m_{g_1} H_{P_1}{}^T + m_{g_2} H^T{}_{P_2 s}\right) D^T{}_{ii_1} C_1 (1 + \delta)$$

$$A_{31} = m_{g_2} z_{P_2 g_1} h^T D^T{}_{ii_1}$$

$$A_{32} = e_1{}^T \left(I_{g_1} D_{sg_1} + D^T{}_{g_1 g_2} I_{g_2} D_{ii_1}\right)$$

$$A_{33} = I_{XXg_1} + e_1{}^T D^T{}_{g_1 g_2} I_{g_2} D_{g_1 g_2} e_1$$

$$A_{34} = e_2{}^T I_{g_2} D_{g_1 g_2} e_1$$

$$A_{35} = - m_{g_2} z_{P_2 g_1} h^T D^T{}_{ii_1} C_1 (1 + \delta)$$

$$A_{42} = e_2{}^T I_{g_2} D_{ii_1}$$

$$A_{43} = e_2{}^T I_{g_2} D_{g_1 g_2} e_1$$

$$A_{44} = I_{YYg_2}$$

REFERENCES

1. Anderson, W. W.; and Joshi, S. M.: The Annular Suspension and Pointing (ASP) System for Space Experiments and Predicted Pointing Accuracies. NASA TR R-448, 1975.

2. Hendricks, T. C.; and Johnson, C. H.: Stochastic Crew-Motion Modeling. J. Spacecraft and Rockets, vol. 8, no. 2, Feb. 1971, pp. 150-154.

3. R. A. Marmann: An Evaluation of the Attitude Measurement System for the Spacelab IPS. Memo dated Aug. 5, 1975. NASA--George C. Marshall Space Flight Center, Huntsville, Alabama.

4. Smith, P. G.: Numerical Solution of the Matrix Equation $A X + X A^T + B = 0$. IEEE Trans. Automat. Contr. vol. AC-16, no. 3, June 1971, pp. 278-279.

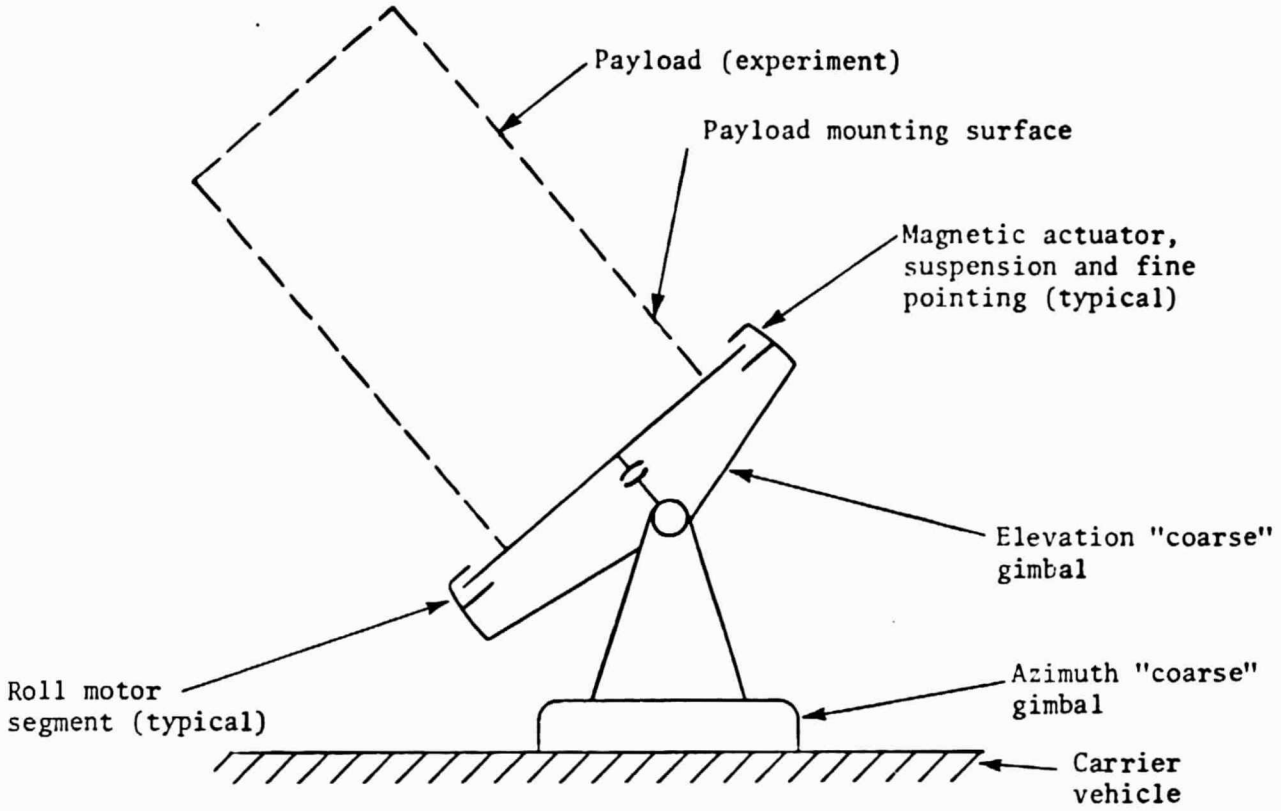

(a) Azimuth-elevation gimbal configuration.

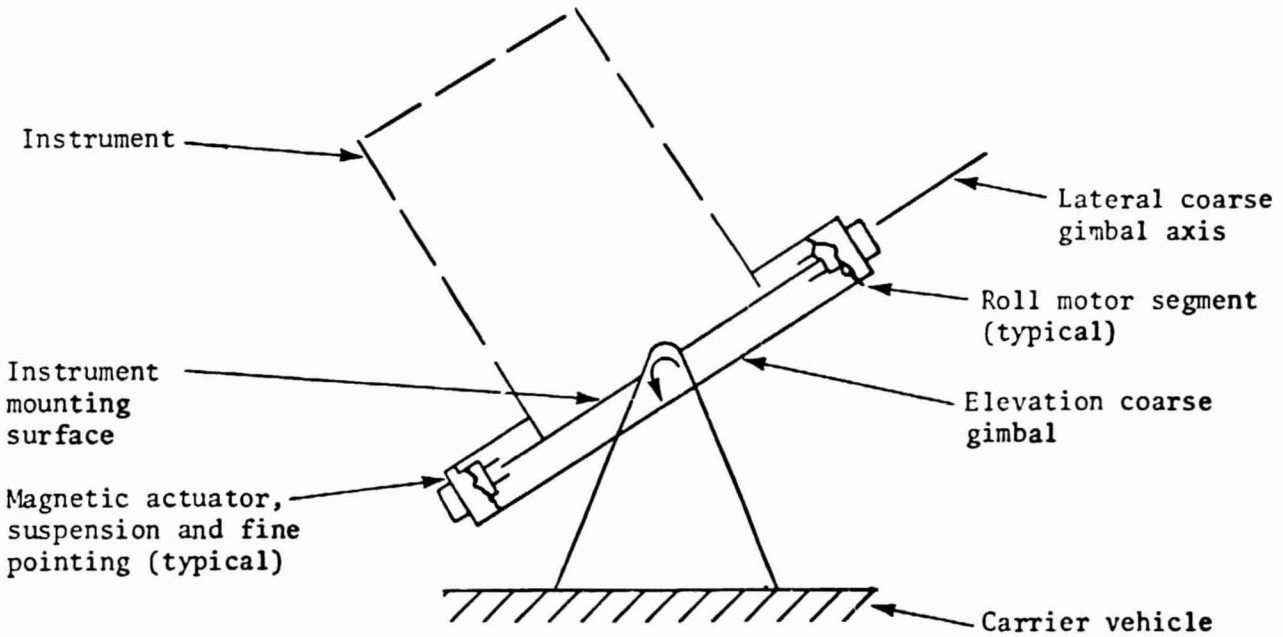

(b) Elevation-lateral gimbal configuration

Figure 1. Annular Suspension and Pointing (ASP) System

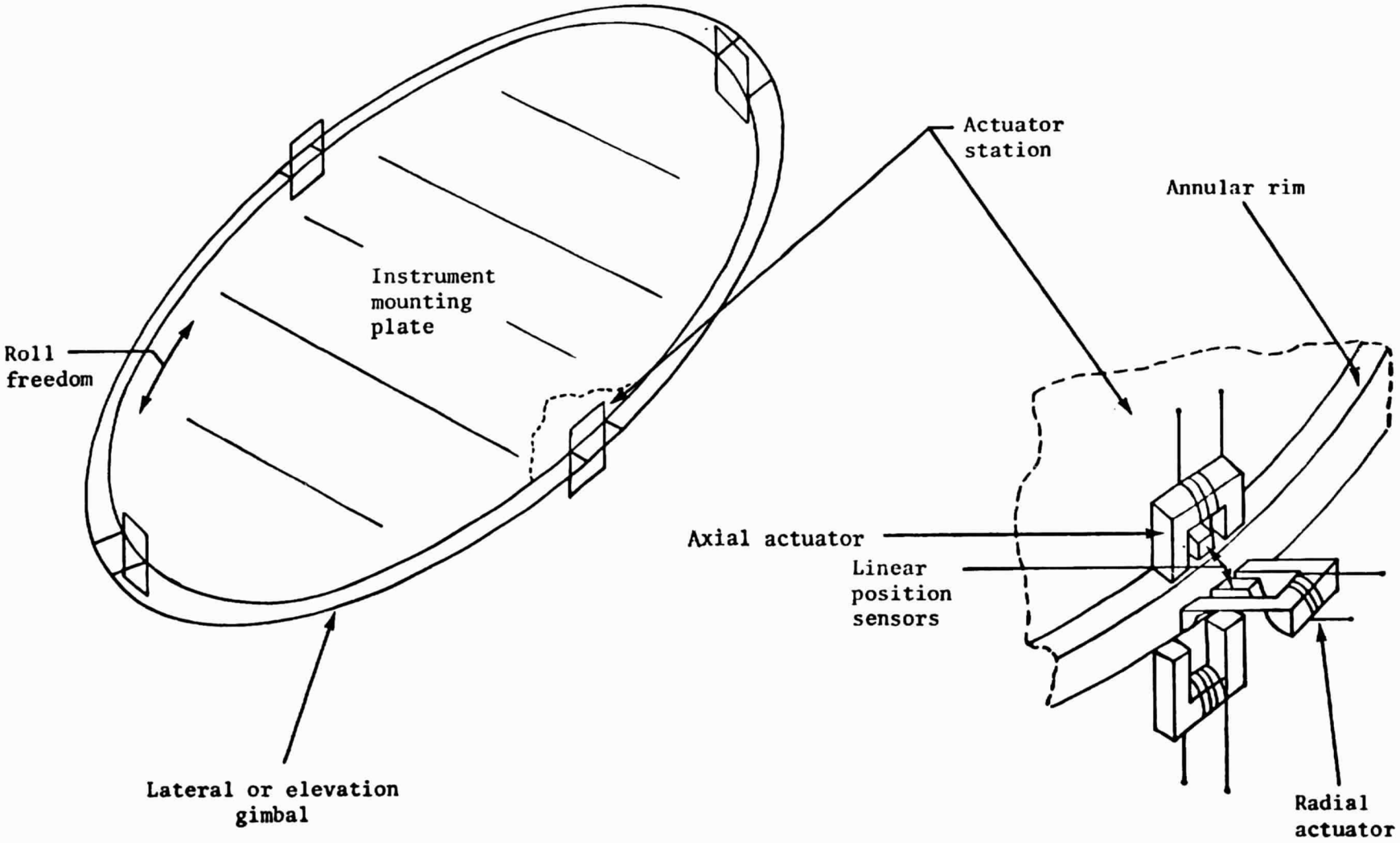

Figure 2. Vernier Pointing Assembly Configuration

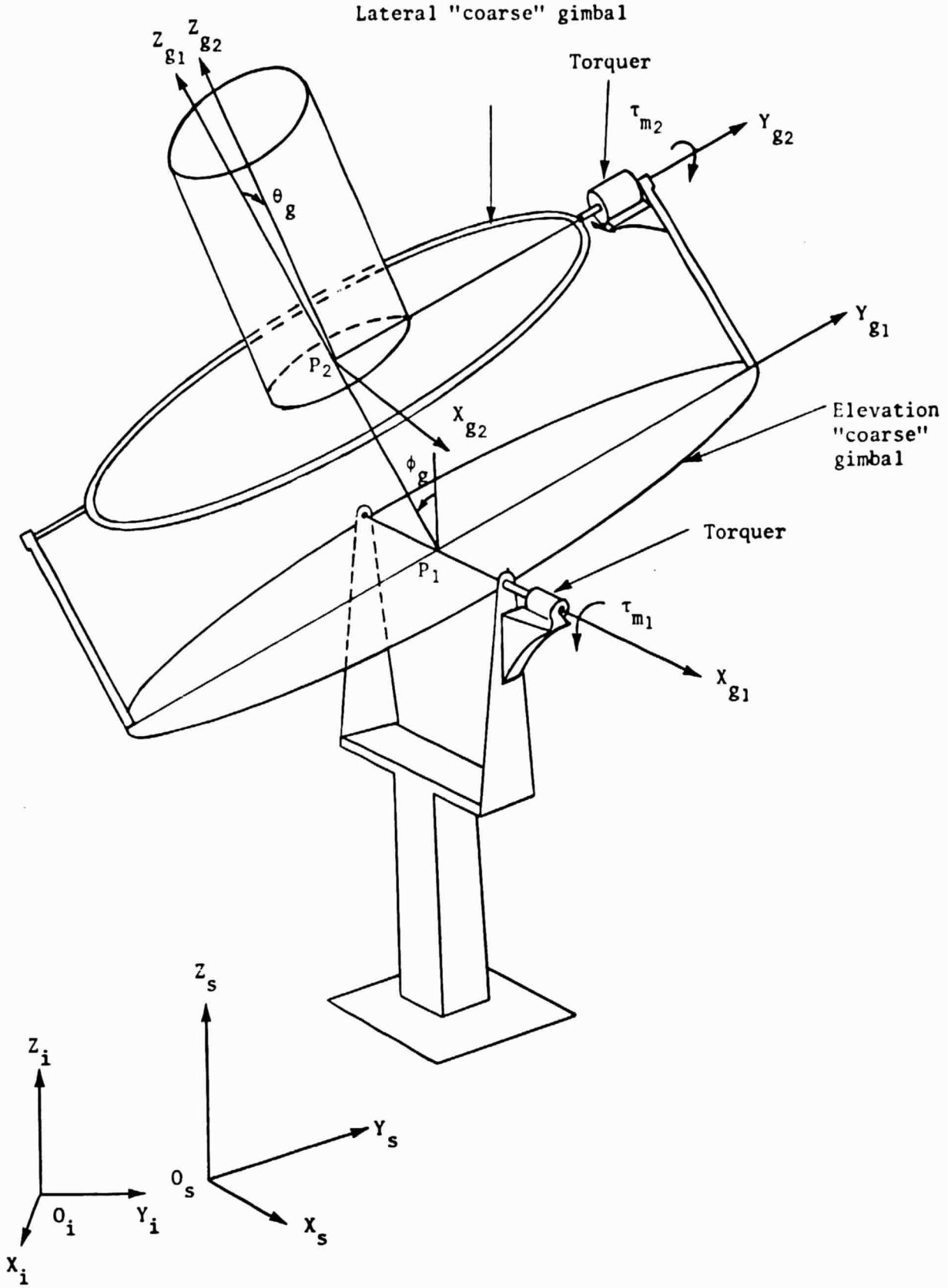

Figure 3. Details of Coarse Pointing Assembly

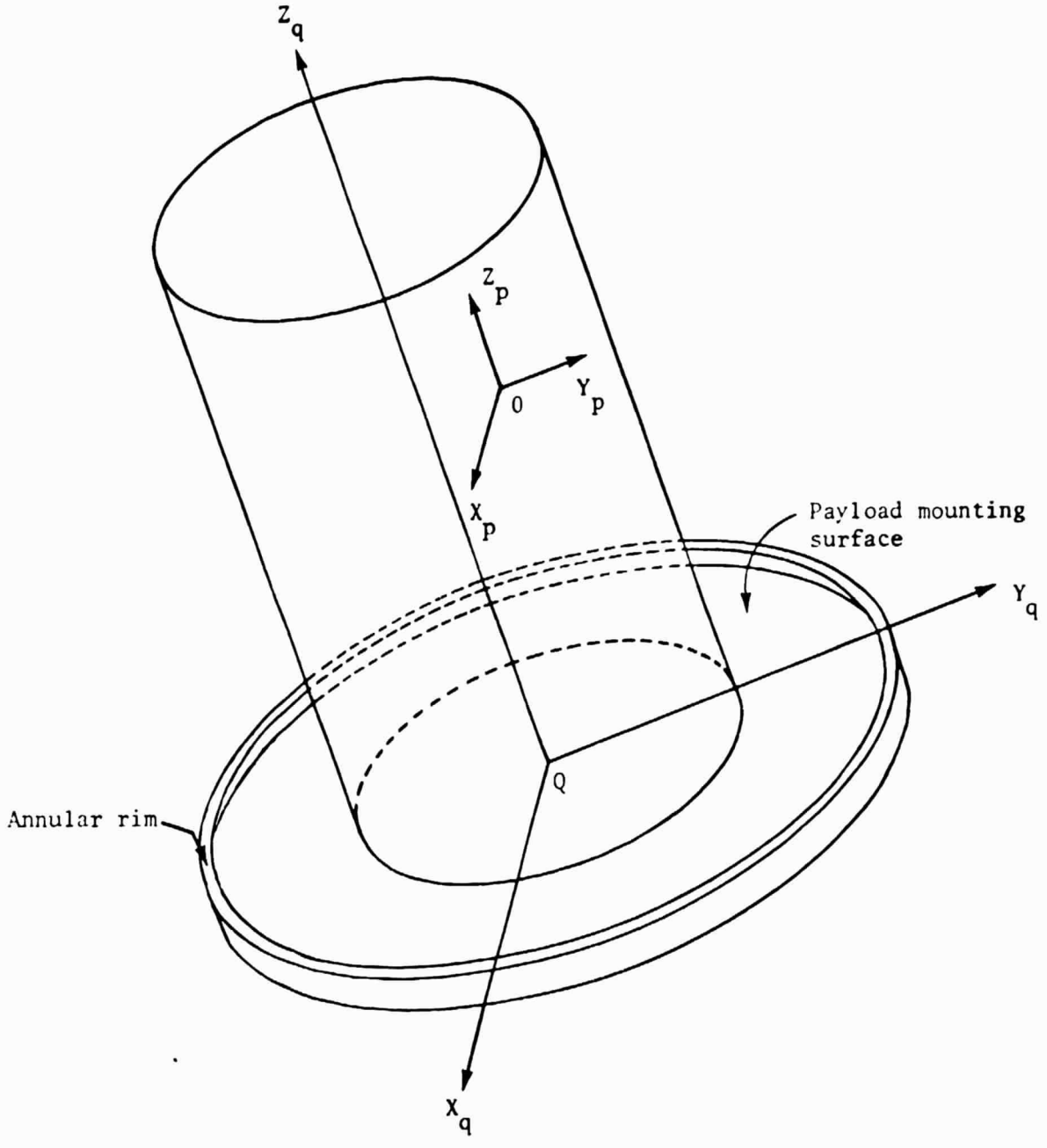

Figure 4. Payload Assembly